Powder Technology 399 (2022) 117011

Contents lists available at ScienceDirect

Powder Technology

journal homepage: www.elsevier.com/locate/powtec

Bed symmetry in the fountain confined conical spouted beds with open-sided draft tubes

Mikel Tellabide *, Idoia Estiati, Aitor Atxutegi, Haritz Altzibar, Javier Bilbao, Martin Olazar

Department of Chemical Engineering, University of the Basque Country UPV/EHU, P.O. Box 644, E48080 Bilbao, Spain

ARTICLE INFO

Article history:
Received 3 June 2021
Received in revised form 8 October 2021
Accepted 22 November 2021
Available online 26 November 2021

Keywords:
Fine particles
Particle velocity
Spout shape
Fountain core
Conical spouted bed
Fountain confiner

ABSTRACT

Bed symmetry has been analysed in fountain confined conical spouted beds operating with fine particles. Thus, vertical particle velocities and the spout shape have been determined in a wide range of spouting air velocities and bed configurations. Bed symmetry is widely accepted in the spouted beds without draft tubes or with non-porous ones, but this is not the case when open-sided draft tubes are used. Thus, radial particle velocity profiles differ depending on the cross-sectional angular plane considered in the open-sided draft tubes. The spout expands preferentially along the tube opened surface, and is wider as spouting air velocity and aperture ratio are increased. The literature correlations proposed for the average spout diameter have been analysed and no one is valid for estimating this parameter in the whole range of spouting air velocities and configurations analysed in these systems operating with fine particles.

1. Introduction

The spouted bed regime has proven to be a promising gas-solid contact method to overcome the limitations involving other technologies, as are those concerning stable operation with coarse particles (greater than 1 mm) in a fluidization regime. Nevertheless, the main present limitation of the spouted bed technology concerns its scaling to industrial level, especially in processes involving fine particle operation [1,2]. Although tools like CFD modelling [3] and artificial neural networks [4] have been used to delve into the understanding of complex and highly non linear systems, as are spouted beds, the gas-solid interaction and fluid motion in these beds are still unraveled.

In order to attain a suitable operation and optimal design of the spouted bed in relevant applications, such as drying [5], combustion [6], pyrolysis [7] or steam gasification [8], knowledge of particle circulation rate and particle velocity distribution is required for understanding and controlling the operation and maximizing product yield. Unfortunately, the aforementioned computational tools depend on the availability of experimental data about these systems, which may exhibit highly unsteady and complex hydrodynamic behaviour [9].

Spouted bed hydrodynamic characterization has been improved in recent years by monitoring detailed flow structures inside the reactor, apart from the overall system pressure drop data. Thus, there is an extensive variety of particle tracking methods in the literature, which are commonly classified into intrusive and non-intrusive methods. The former account for the older ones, such as those based on piezoelectric [10] or optical fiber probes [11]. These techniques require the insertion of the probe to the measuring point, which may cause a local disturbance of the solid movement [12–14]. Accordingly, a variety of non-intrusive particle tracking methods have been developed and tuned, such as radioactive particle tracking [15], particle image velocimetry [16] or X-ray computed tomography [17], which may provide full-field flow measurements. Nevertheless, non-intrusive methods are generally more complex and expensive than intrusive ones, and involve additional complexity in the experimentation, as they may involve special safety procedures [18] and interference in the measurements [19].

Intrusive methods make it possible to measure spouted bed features, such as the spout evolution form the bottom to the surface of the bed or the local solid oscillatory movement. Information about the spout zone size and shape is of high relevance for a better understanding of the spouted beds technology, since it accounts for a significant fraction of the bed volume and has a crucial influence on the solid and gas flow patterns [20]. The first spout measurements were based on visual observation through the transparent wall in half-column or two-dimensional contactors [10,21–23]. Thus, Mikhailik et al. [10] measured the spout diameter at different bed levels in half and full cylindrical columns, using a piezoelectric technique in the the latter, and reported that both spout shapes were quite similar. Nevertheless, Benkrid et al. [24] and He

* Corresponding author.
E-mail address: mikel.tellabide@ehu.eus (M. Tellabide).

https://doi.org/10.1016/j.powtec.2021.11.055

et al. [25] measured the spout diameter using an optical fiber probe and stated that the wall effect significantly distorts the spout shape.

It is well-established in the literature that solid flow in the annulus is axisymmetric [17,26], and particle velocities are therefore measured at a single radial plane [25]. Accordingly, although the diameter of the spout varies from the bed bottom to the surface, its cross-sectional shape is assumed to be circular [9]. The only studies dealing with non-axisymmetric flow patterns are those involving half-columns [24,25] and vortex generators [27].

The open-sided draft tubes are interesting devices because they greatly improve the gas-solid contact due to their lateral opened surface [28], as well as ensure spouting stabilization. Moreover, the fraction of the gas that percolates from the spout into the annulus enhances the overall solid circulation in the annulus, especially close to the opened surface of the draft tube. This fact suggests that, at a given bed level, the particle velocity profile from the spout axis to the bed wall depends on the angular coordinate. On the one hand, there is a continuous profile along the angular coordinate passing through the opened fraction of the draft tube and, on the other hand, there is a discontinuity at the draft tube wall in the profile along the angular coordinate passing through the closed fraction of the draft tube.

Therefore, the aim of this work is to analyze bed and spout symmetry in fountain confined conical spouted beds operating with fine particles. Accordingly, vertical particle velocities have been measured using Particle Tracking Velocimetry (PTV), and the radial profiles of particle velocity, as well as the shape and size of both the spout and the fountain core, have been determined. Moreover, average spout diameters have been calculated for different configurations and air velocities, and compared with the theoretical values determined using literature correlations.

2. Experimental

2.1. Equipment and materials

Fig. 1 shows the pilot plant used in this study, which is composed of a blower, flowmeter, pressure drop gauge, contactor, filter and cyclone, and has been detailed in a previous paper [29]. A conical contactor (Fig. 2a) made of polyethylene terephthalate has been used with the following dimensions: column diameter (D_C), 0.36 m; contactor angle (γ), 36°; height of the conical section (H_C), 0.45 m; base diameter (D_i), 0.062 m. Moreover, the static bed height (H_0) and inlet diameter (D_0) used are 0.20 m and 0.04 m, respectively.

Stable operation with fine particles requires the use of a fountain confiner (Fig. 2a), which is placed above the bed and confines the particles in the fountain. This internal device is a cylindrical tube made of polyethylene terephthalate with the upper end closed to avoid gas and solid leaving the contactor through the top of the confiner. Furthermore, it is provided with a cone shaped cap on the outer top surface to avoid solid deposition. The main dimensions of the fountain confiner are as follows: length of the confiner cylindrical body (L_F), 0.50 m; internal diameter of the confiner (D_F), 0.20 m; distance between the lower end of the device and the bed surface (H_F), 0.06 m.

Different draft tubes of cylindrical shape have been used. These devices are made of stainless steel and are fitted to the inlet of the conical section and placed along the contactor axis. Two types of draft tubes have been used, namely, open-sided (Fig. 2b) and nonporous (Fig. 2c) ones. Their main characteristic factors are as follows: length of the tube (L_T), 0.20 m; height of the entrainment zone (distance between the gas inlet nozzle and the lower end of the tube) (L_H), 0.07 m; and aperture ratio (AR), i.e., the fraction of the lateral surface area opened for gas and solid interchange, 42, 57 and 78%.

All the runs have been carried out operating with fine siliceous sand particles of 0.246 mm average particle diameter and 2390 kg m^{-3} solid density. The former has been determined using mesh sizes of 0.2 and 0.3 mm in a CISA RP 200 N sieve shaker, and has been confirmed by laser diffraction particle size analysis in a Mastersizer 2000. The solid density has been determined in an Autopore 9220 mercury porosimeter from Micromeritics.

2.2. Experimental procedure

An optical set-up composed of a high speed camera (AOS S–PRI, AOS Technologies AG) and a borescopic system has been used to obtain vertical particle velocities. The camera provides a maximum recording resolution of 900 × 700 pixels with a speed of 16500 frames per second at

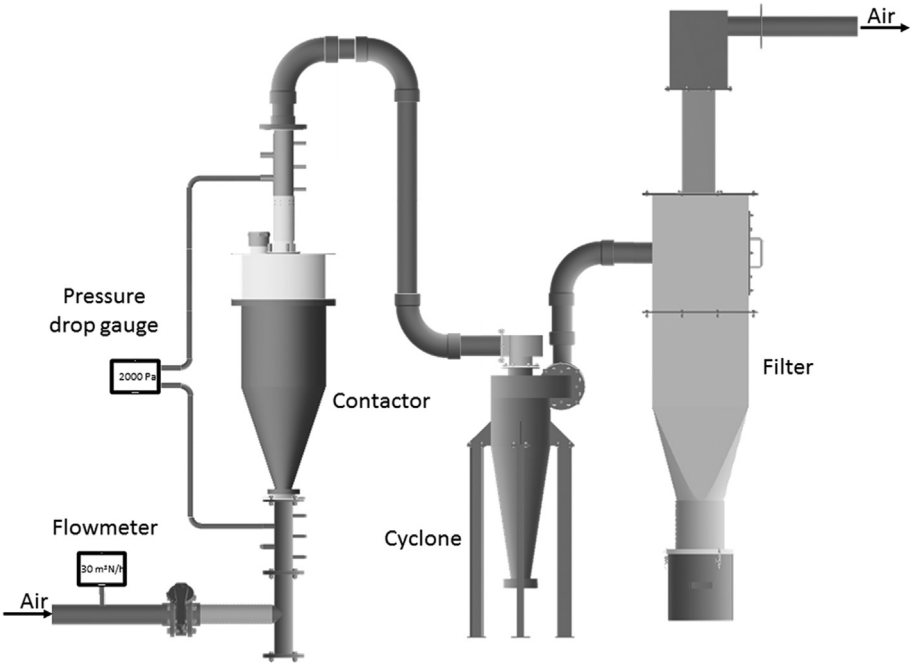

Fig. 1. Diagram of the pilot scale plant.

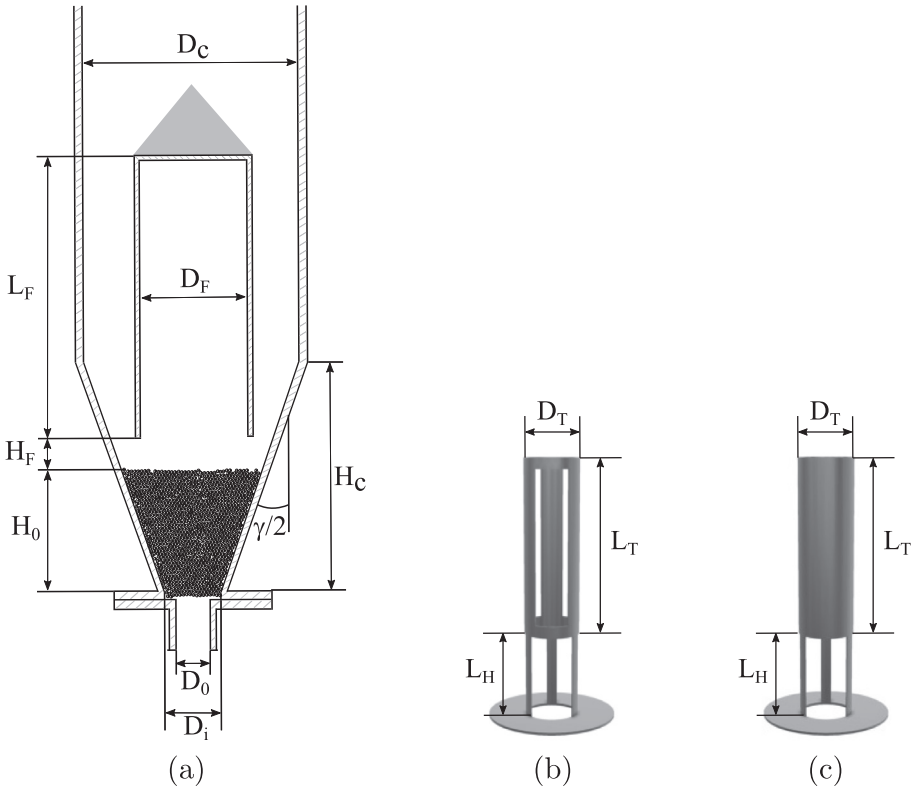

Fig. 2. Geometric factors of (a) the conical contactor and fountain confiner, and (b) open-sided and (c) nonporous draft tubes.

reduced resolution. The borescope is connected to a continuous light source to brighten the front area of the borescope tip, and the whole optical set-up is displaced by a set of sliders in order to position the borescope tip at any point inside the contactor. All the recordings by the optical set-up are taken in front of the borescope tip, which reduces solid flow disturbances at the measuring point, as perturbations may only be due to the stem of the boroscope. A detailed description of the optical set-up can be found in a previous paper [30].

Measurements have been carried out by positioning the borescope tip at the contactor or confiner wall and displacing it step-by-step in the radial direction every centimetre up to the contactor axis. The radial particle velocity profiles attained at different measuring heights show negative and positive values. The former correspond to the annular and fountain periphery, and the latter to the spout and fountain core. Thus, as shown in Fig. 3, the radial points where particle velocity is zero correspond to the spout-annulus interface in the bed (Fig. 3a) and core-periphery interface in the fountain (Fig. 3b). Given that the position of both interfaces highly depends on the inlet air flow rate, the study has been carried out at the minimum spouting velocity and air velocities well above the minimum one. Thus, the spouting regimes analyzed in each configuration correspond to the following spouting velocities: u_{ms} (3.86 m s^{-1}) and 3.31u_{ms} without tube; u_{ms} (3.42 m s^{-1}), 2.35u_{ms} and 6.40u_{ms} when open-sided tubes are used; and u_{ms} (2.54 m s^{-1}), 2u_{ms}, 3u_{ms} and 8.60u_{ms} when the nonporous draft tube is used.

When open-sided tubes are used, both gas percolation from the spout into the annulus and solid cross-flow from the annulus into the spout depend on the opened fraction of the tube surface. Accordingly,

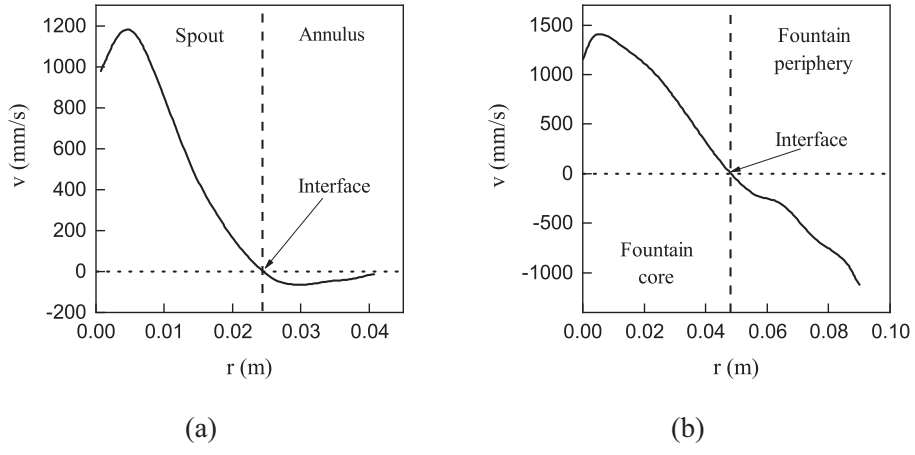

Fig. 3. Delimitation of the interface based on the particle velocity profile. (a) Spout-annulus interface in the bed and (b) core-periphery interface in the fountain.

open-sided tubes differing in the aperture ratio (AR) have been used in a wide range of air velocities, from the minimum one to 22 m s^{-1}, in order to measure the spout expansion and its shape (symmetry). Radial particle velocity profiles have been been obtained for each configuration at the three angular coordinates shown in Fig. 4. One along the angular coordinate from the axis to the wall passing through the midpoint of the draft tube aperture (line corresponding to 0°, Fig. 4), another one along the angular coordinate touching the edge of the draft tube wall (lines corresponding to 48°, 36° and 30° for the aperture ratios of 78, 57 and 42%, respectively, Fig. 4), and the third one for the angular coordinate from the axis to the wall passing through the midpoint of the draft tube wall (line corresponding to 60°, Fig. 4). Therefore, the angular coordinates through the midpoint of the aperture and through the midpoint of the draft tube wall are the same in all the configurations. Nevertheless, the angular coordinate touching the edge of wall differs depending on the aperture ratio. In order to simplify the experimental procedure, the cross-sectional spout shape has been delineated by polynomial interpolation between the three points mentioned above. This assumption has been verified with a few measurements carried out in the midway positions between the three points. Velocity measurements at different radial positions have been carried out at four bed levels from the bottom to the surface of the bed, which are 0.03, 0.11, 0.15 and 0.20 m. Furthermore, symmetry is accepted in the fountain zone, so measurements have been conducted along a single angular coordinate at four levels from the bottom to the top in this zone, which are 0.24, 0.30, 0.53 and 0.73 m.

A total of four recordings (replicates) were carried out at each measuring point and the whole process was repeated at least twice in order to obtain reliable results. The recorded images were introduced into a solid detection algorithm where particles were located and paired in consecutive frames. Spouted bed systems are characterized by severe spatial gradients in both particle velocity and voidage [31], which leads to great differences in the images captured in the dense (annulus) and dilute zones (spout/fountain). In the images obtained in the dense zone, single particle detection is no feasible because they descend in a moving bed. Nevertheless, a previous study proved that Farneback pyramidal algorithm [32] from OpenCV may accurately detect overall particle edges. In the case of the dilute zone, the image was treated applying a dynamic histogram equalization and a canny edge detector. Therefore, particles are identified as close regions and their centroid positions are calculated. This routine was repeated for each frame and particles were paired in consecutive frames minimizing the total solid displacement. Based on this procedure, single and overall particle velocities are calculated for each frame, which allow determining the average vertical particle velocity at each measuring point with an error below 10%. [30].

3. Results

3.1. Radial profiles of particle velocity in the configurations with open-sided draft tube

Fig. 5 shows the radial profiles of particle velocity along the angular coordinates analysed at the bed level of $H_0 = 0.20$ m when spouting was carried out by feeding two inlet flow rates (minimum and 6.40 times the minimum one) in the configuration with an open-sided draft tube of 57% aperture ratio (AR).

As shown in Fig. 5, the trend of the radial profile of particle velocity varies depending on the angular coordinate in the radial plane. Thus, independently of the inlet flow rate, particles moving downwards in the annulus along the angular coordinate passing trough the midpoint of the draft tube opened fraction (0°) have similar profiles to those reported in the literature [33–36], i.e., downward velocity peaks (inverse peak) at an intermediate position in the annulus. Although some authors stated that the peak position is close to the spout-annulus interface, it depends on the operational conditions and reactor geometric parameters. A very interesting fact is the great spout expansion along this angular plane passing through the middle of the draft tube opened space, especially when operation is carried out at high air velocity. Thus, as observed in Fig. 5b, the spout diameter ranges from the axis to the radial position corresponding to zero particle velocity (approximately $r/R = 0.6$), i.e., the size of the spout in this angular plane is approximately three times the tube diameter. Furthermore, the highest downward particle velocities in the annulus half on the wall side are those corresponding to the angular coordinate passing though the midpoint of the opened slot of the draft tube (0° coordinate).

Similar profiles to those mentioned above are obtained for the angular coordinate passing through the edge of the draft tube wall (36°), even though the decrease in particle velocity near the tube is smoother at the minimum spouting velocity due to the lower gas percolation from the spout into the annulus along this radial plane. However, at high air velocity (Fig. 5b), gas percolation is higher than when operating at u_{ms} and similar profiles as those obtained along the 0° angular coordinate are obtained. Furthermore, the great expansion of the spout is also noteworthy. Finally, similar profiles are observed along the 60° angular coordinate (from the wall of the draft tube to the wall of the contactor) when operation is carried with either low or high air velocity. In these cases, the downward particle velocity decreases to a given value in the vicinity of the tube (peak), it then increases and peaks (inverse peak) at an intermediate position in the annulus, and finally decreases towards the contactor wall. The peaks are more pronounced at the minimum spouting velocity (Fig. 5a), whereas the overall particles velocities are much higher at the higher flow rate

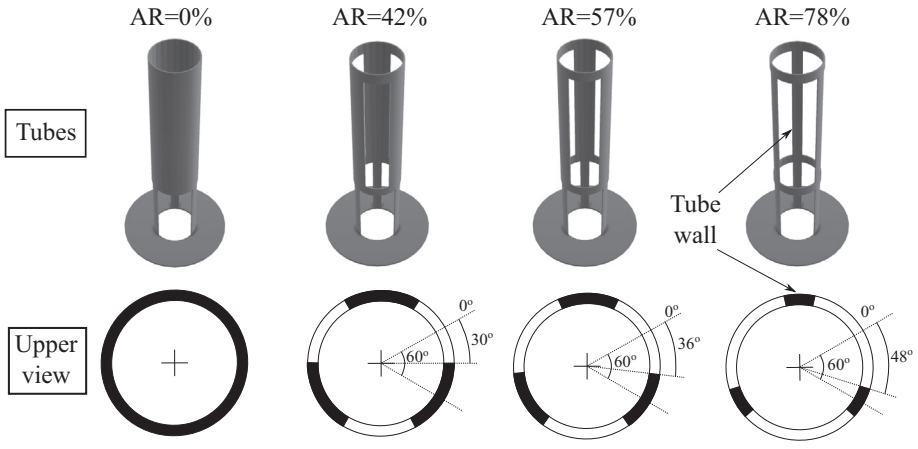

Fig. 4. Draft tubes used in the experimentation, with their corresponding upper view, and the angular coordinates along which vertical velocities were measured.

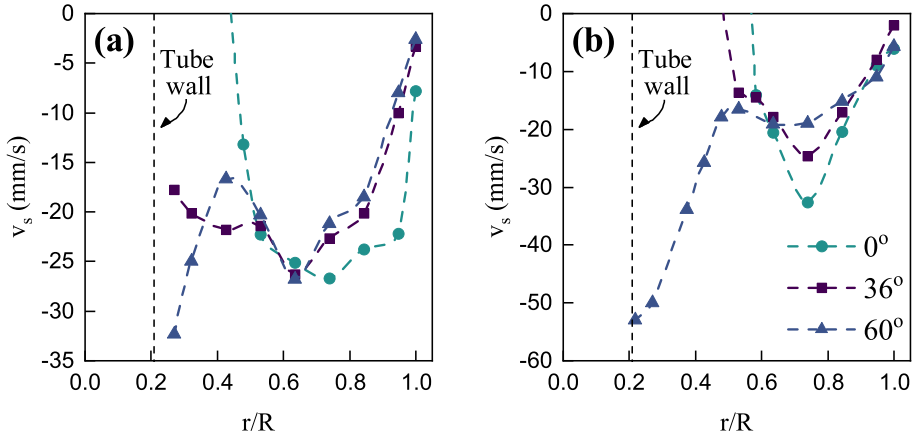

Fig. 5. Radial profiles of particle velocity along different angular coordinates at the bed level of $H_0 = 0.20$ m in the annulus of a spouted bed provided with an open-sided tube of 57% AR and operating at (a) the minimum spouting velocity (u_{ms}) and (b) 6.40 times the minimum one.

(Fig. 5b). The spout expansion in the opened fraction of the tube is much more pronounced for the higher flow rate.

Overall, downward particle velocities in the annulus half closer to the wall are the highest along the 0° angular coordinate, but no clear trend is observed at low r/R values. Nevertheless, as shown in Fig. 5, a great spout expansion occurs along the opened surface of the tube, especially at high air velocities.

Fig. 6 shows the radial profiles of particle velocity along the different angular coordinates for the spouted beds equipped with open-sided draft tubes of 78% and 42% aperture ratios operated at high air velocity.

Unlike the different trends obtained with the tube of 57% AR (Fig. 5b), the radial profiles along all the angular coordinates follow the same trend when the tube of highest AR, i.e., 78%, is used (Fig. 6a). This result means that, at high air velocity, the spout expands out of the tube limits at all the angular planes. In fact, the tube has been swallowed by the spout. Furthermore, the extension of the annular zone in front of the opened surface of the tube (0° coordinate) decreases significantly. Thus, the length of the annulus on the bed surface only accounts for 20% of the total bed surface radius, i.e., from $r/R = 0.8$ to 1, Fig. 6a. Concerning downward particle velocities in this configuration, they are similar along the angular coordinates of 48° and 60°, which in turn are much higher than those along 0° coordinate. This is a consequence of the spout expansion and air percolation from the spout into the annulus through the opened area of the tube, which leads to an overall decrease in the downward particle velocity in the annulus.

A decrease in the opened fraction of the draft tube to 42%, Fig. 6b, leads to similar trends as those mentioned for 57% aperture ratio, Fig. 5b, i.e., the spout does not expand beyond the non-opened fraction of the tube. Furthermore, the inverse peaks observed for the angular coordinates through the opened fraction (0° and 30°) are less pronounced than those obtained with 57%. Accordingly, the tube with 42% AR leads to the lowest symmetry in the spout shape among the three open-sided tubes studied.

3.2. Cross-sectional spout geometry

As reported in a previous paper [36], a three-pointed star spout shape is observed when the open-sided draft tube of 57% AR is used at the minimum spouting velocity, which is consistent with the profiles shown above (Figs. 5 and 6). Fig. 7 shows the cross-sectional spout shapes obtained using open-sided draft tubes of different aperture ratio and without draft tube at high air velocity, 22 m s^{-1} and 12.78 m s^{-1}, respectively.

As previously mentioned, bed axisymmetry has been assumed when the operation has been carried out without draft tube. Nevertheless, the use of an open-sided tube leads to partial axisymmetry, in which the shape changes depending on the aperture ratio and operating conditions. Thus, as shown in Fig. 7a, a circular spout shape is observed for the configuration without tube, with its diameter being larger as the the longitudinal position is higher. Castellana et al. [37] reported that

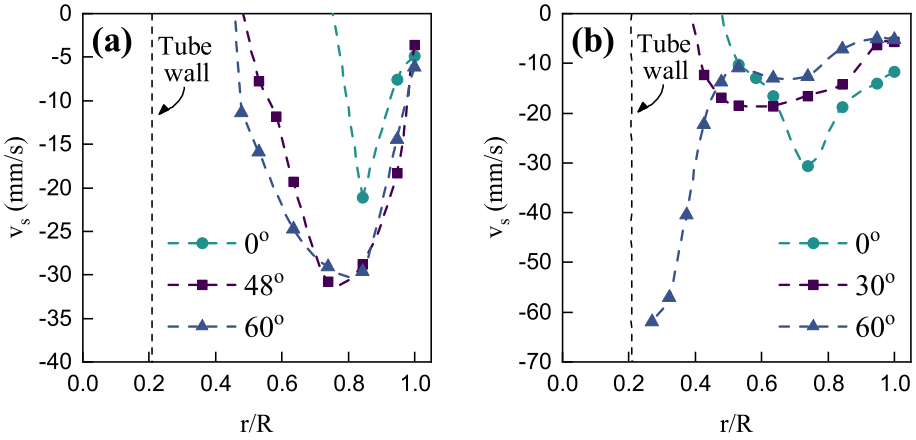

Fig. 6. Radial profiles of particle velocity along the angular coordinates analyzed at the bed level of $H_0 = 0.20$ m in the annulus of a spouted operated at high velocity ($6.40u_{ms}$) with open-sided draft tubes of (a) 78% and (b) 42% aperture ratios.

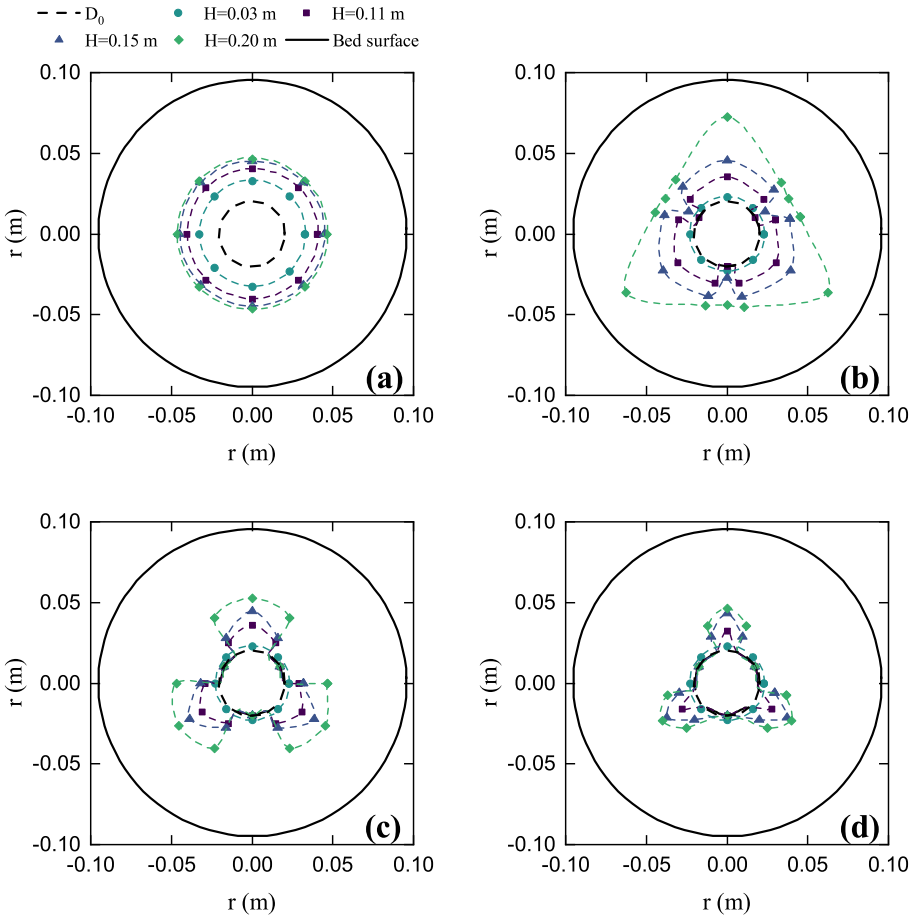

Fig. 7. Cross-sectional spout shape at high air velocity for the configurations (a) without draft tube (100% AR), and with open-sided tubes of (b) 78%, (c) 57% and (d) 42% AR.

spout diameter increases slightly from the inlet to the top of the bed, whilst Olazar et al. [38] stated that the diameter on the upper surface of the bed may be up to three times the contactor inlet diameter. The spout expansion measured in this study is intermediate between those reported by the previous authors (2.3 times the inlet diameter), which confirms that the spout shape and width depend on the operating conditions and contactor geometric factors.

However, when open-sided draft tubes are used, the spout expands out of the draft tube through the opened face (Figs. 7b-7d), with the expansion being proportional to the aperture ratio. As shown in Fig. 7b, the open-sided tube of highest AR leads to a great spout expansion. In fact, on the bed surface the spout swallows the tube, with its shape being triangular. Furthermore, the spout expands significantly all over the bed length, except in the zones where the draft tube is not opened.

The other open-sided tubes lead to similar trends, Figs. 7c-7d, with the spout expansion being lower as the aperture ratio is lower. Furthermore, there is no expansion in the zone in which the tube wall is not opened. The cross-sectional shape of the spout changes from approximately a clover shape to a three pointed star as the aperture ratio is decreased.

3.3. Effect of the air velocity on the spout and fountain core expansion

As shown in Fig. 5, inlet gas velocity greatly affects particle velocity and spout expansion. Accordingly, the spout-annulus interface, as well as the core-periphery interface in the fountain, have been delineated at different air velocities for all the configurations studied (Fig. 8). These interfaces have been determined by locating the null particle velocity along each radial profile on the different measuring heights in the bed (spout-annulus) and fountain (core-periphery). It is noteworthy that the spout-annulus interfaces plotted in Fig. 8b correspond to the maximum expansion through the opened faces (0°) of the open-sided draft tube.

As shown in Fig. 8, the spout and fountain core shapes vary depending on the configuration used. Overall, an increase in air inlet velocity leads to an increase in the size of the spout and fountain core. This trend has already been reported in the literature, especially for the spout [25,39–43], but there is hardly any work dealing with the fountain core expansion. To our knowledge, Olazar et al. [44] and San José et al. [45] are the only authors who reported the effect of the inlet air velocity on the fountain core expansion. They state that an increase in air velocity makes the fountain core become elongated.

In the configuration without draft tube, Fig. 8a, the spout shows a pronounced expansion near the contactor inlet, and a slight and steady expansion further up in the bed. This steady expansion is more severe as the inlet air velocity is increased. Unlike most of the studies reported in the literature [25,9,38,40,42,46–48], Fig. 8a does not show any neck at an intermediate bed level in the spout, but the spout shape is similar to those reported by Djeridane et al. [34] and Mukhlenov and Gorshtein [49]. However, the fountain core shows a neck on its bottom (close to the bed surface). As air velocity is increased, the expansion of the fountain core is more pronounced and takes almost the whole confiner diameter in the upper half of the device.

When the open-sided tube configuration is used, Fig. 8b, the spout hardly expands in the lower half of the bed, but the expansion occurs mainly in the upper half. This fact is explained by the effect of the entrainment zone ($L_H = 0.07$ m), where the spout size hardly changes, but air percolation in this zone makes bed expansion to be significant in the upper half of the bed above. Nevertheless, an increase in air velocity hardly changes the spout size. In the case of the fountain, a

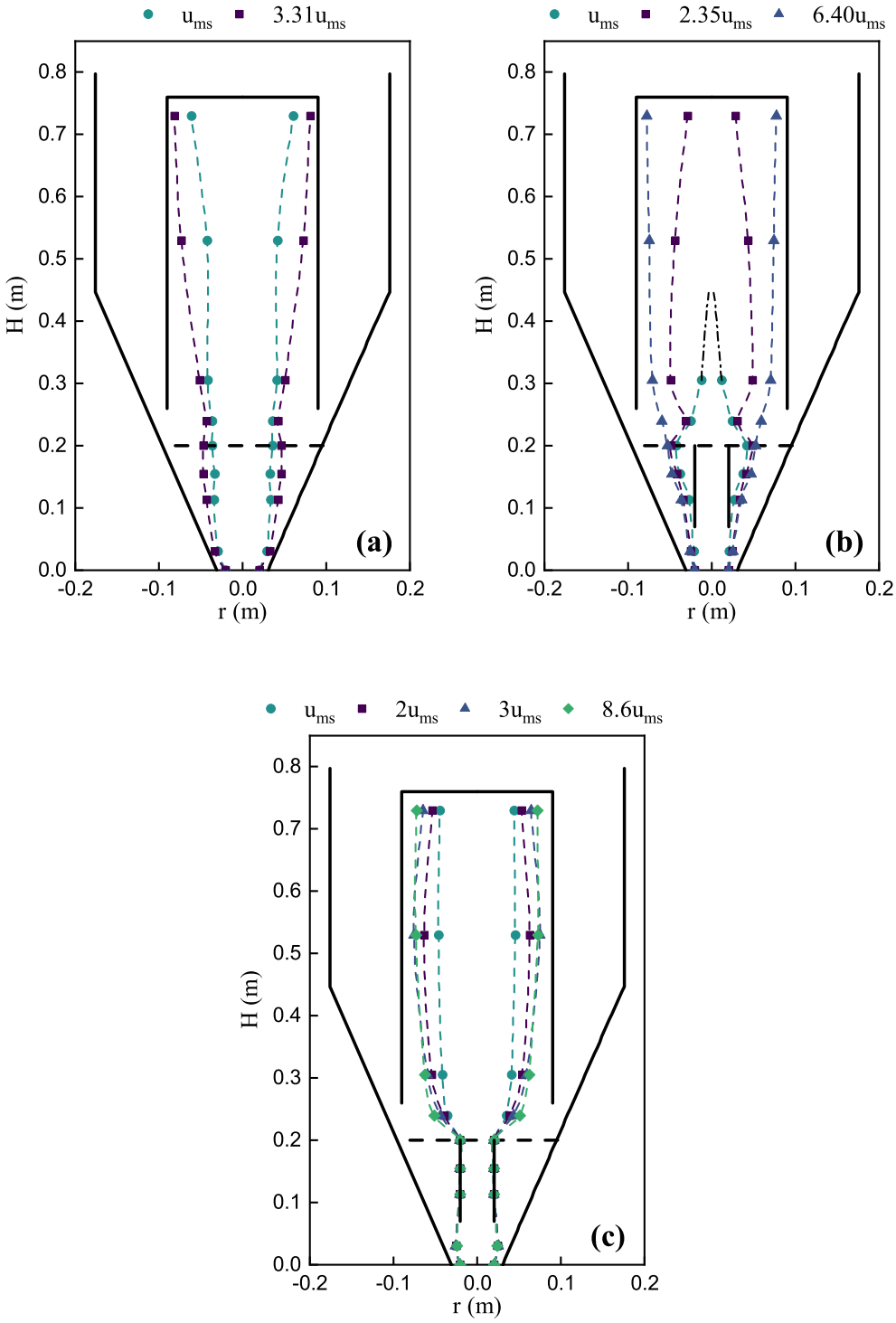

Fig. 8. Spout-annulus interface in the bed and core-periphery interface in the fountain at different air inlet velocities for the configurations (a) without tube, (b) with open-sided tube of 57% AR and (c) nonporous one.

moderate increase in gas velocity ($2.35u_{ms}$) leads to an increase in the fountain height to the top of the confiner. Furthermore, a very pronounced neck in the fountain core occurs close to the bed surface when operation is carried out at both u_{ms} and $2.35u_{ms}$, which is due to the high amount of particles descending in the fountain periphery at this height. Although the fountain reaches the top of the confiner when velocity is increased from the minimum one to 2.35 times the minimum one, there is a slight contraction in the fountain core at its top, which is a consequence of the decrease in particle velocity at the upper surface of the confiner. Furthermore, the fountain core expands greatly when a high air velocity ($6.40u_{ms}$) is used and takes almost the whole confiner volume.

Finally, Fig. 8c shows the spout and fountain core evolution for different air velocities when the nonporous draft tube is used. In this case, a similar spout evolution along the bed height is observed for all air velocities. There is a slight spout expansion at the bed bottom, and the air runs then through the nonporous draft tube. Thus, almost the whole spout interface (except along the entrainment zone) is delimited

by the tube wall for all air velocities. Nevertheless, a very pronounced fountain core expansion occurs just above the bed surface or upper end of the draft tube, which may be due to the increase in the cross-sectional area available for the air. The fountain core expands slightly until approximately the middle section in the confiner, and it then undergoes a slight contraction until the top of the confiner. This trend in the confiner is slightly more pronounced as air velocity is increased. Similarly as in the configuration with the open-sided draft tube, most of the confiner volume is taken by the fountain core when high air velocities are used.

3.4. Average spout diameter

As shown in Figs. 7 and 8, the spout shape and size are conditioned by the configuration and inlet air velocity used. Accordingly, average spout diameters have been calculated for different configurations and air velocities, and have been compared with the literature correlations. Nevertheless, in the configuration with the nonporous tube there is hardly any expansion and the spout diameter is the inlet diameter itself.

As reported in a previous work [36], most of the literature correlations have been developed for coarse particles operated at the minimum spouting velocity and they under-predict the average spout diameter for fine particle beds operated with fountain confiner. Only those reported by San José et al. [47] and Volpicelli et al. [50] provide reasonable results (error below 10%). Table 1 shows the correlations in the literature allowing reasonable predictions under certain conditions.

Table 1 evidences the lack of a suitable literature correlation for predicting the average spout diameter of fine particle beds in the range of air velocities and configurations of practical interest. Thus, although there are correlations relating the spout diameter with air velocity, the results obtained in this study reveal that they were built for simple configurations and not well parameterized, especially for high air velocities.

The correlations by San José et al. [47] and Volpicelli et al. [50] provide reasonable estimations for all the configurations at the minimum spouting velocity, but the error increases significantly when air velocity is increased. San José et al. [47] used a similar spouted bed configuration to that studied in this work, and they stated that the spout does not undergo a great change when air velocity is increased. This fact is explained by the narrow range of air velocities used in their study, as they used a maximum value of $1.3u_{ms}$, while in the current study this range has been widened to $2 - 8.6u_{ms}$. Volpicelli et al. [50] found a spout shape with two necks and two expansion zones, and the predictions of their correlation are better for the configuration without draft tube than for those with open-sided draft tubes, with deviations being 33% and 50 − 173% respectively.

However, the correlations proposed by McNab et al. [23] and Green and Bridgwater [51] allow better predictions (error <45%) at high air velocities than those aforementioned, but they greatly underestimate the average spout diameter at the minimum spouting velocity. These authors used granular materials, such as wheat and millet, which are bigger than sand, and so they need more drag force to expand the spout. Furthermore, open-sided tubes avoid great spout expansion at high air velocities, which explains the better predictions of their correlations for these configurations than those without tube.

Overall, Table 1 shows that every average spout diameter correlation depends on the operating conditions and contactor geometry. Moreover, all these correlations have been proposed based on the assumption of axisymmetry in the spout shape, i.e., operating only with the configuration without draft tube. Nevertheless, this study shows that the spout shape and size are highly dependent on the aperture ratio, which is a parameter that will have to be considered in any correlation for the prediction of the average spout diameter in the configurations with open-sided tube.

Table 1
Comparison of the experimental average spout diameters with those predicted by different correlations.

Correlation	Configuration	AR (%)	Air velocity (m/s)	$\bar{D}_s$ (m)	$\bar{D}_{s,exp}$ (m)	Error (%)
San José et al. [47]	Without tube	100	3.86	0.050	0.061	18.03
		100	12.82	0.158	0.075	110.1
	Open-sided tube	78	21.88	0.278	0.069	300.93
		57	3.42	0.049	0.045	8.88
		57	8.07	0.111	0.053	111.11
		57	21.88	0.291	0.055	423.03
		42	21.88	0.347	0.048	622.11
Volpicelli et al. [50]	Without tube	100	3.86	0.055	0.061	9.83
		100	12.82	0.100	0.075	33.34
	Open-sided tube	78	21.88	0.131	0.069	89.22
		57	3.42	0.052	0.045	15.55
		57	8.07	0.080	0.053	50.71
		57	21.88	0.131	0.055	135.18
		42	21.88	0.131	0.048	173.12
Green and Bridgwater [51]	Without tube	100	3.86	0.025	0.061	59.01
		100	12.82	0.045	0.075	40.75
	Open-sided tube	78	21.88	0.058	0.069	16.38
		57	3.42	0.023	0.045	48.88
		57	8.07	0.036	0.053	32.73
		57	21.88	0.058	0.055	3.93
		42	21.88	0.058	0.048	20.07
McNab et al. [23]	Without tube	100	3.86	0.023	0.061	62.29
		100	12.82	0.041	0.075	45.64
	Open-sided tube	78	21.88	0.053	0.069	23.28
		57	3.42	0.021	0.045	53.33
		57	8.07	0.033	0.053	38.28
		57	21.88	0.053	0.055	4.65
		42	21.88	0.053	0.048	10.73

4. Conclusions

Spouted beds are commonly considered to be axisymmetric for modelling and simulation purposes. Nevertheless, open-sided tubes allow gas and solid exchange through the opened surface of the tube, which significantly increases aeration in the annular zone close to the opened surface, as well as the solid cross-flow from the annulus into the spout in this zone.

Therefore, the particles on the annulus wall in front of the opened surface have greater downward velocity than those on the wall in front of the closed surface, but the opposite trend is observed close to the interface, i.e., particles have greater velocity on the outside of the closed fraction of the draft tube than on the opened fraction. Moreover, these trends are more pronounced as air velocity is increased. Nevertheless, when high aperture ratios are used the bed tends to become homogenized.

Axisymmetric spout shapes are obtained for the configuration without draft tube, but partially asymmetric shapes are observed in the configurations with open-sided tubes due to the spout expansion through the opened surfaces. Overall, a clover shaped spout is obtained at high spouting velocities, whereas a three-pointed star spout shape is observed at low velocities. It is noteworthy that a triangular spout shape is observed in the upper zone of the bed when open-sided tubes of high aperture ratio are used.

In the configurations without draft tube, the spout expands as air velocity is increased, with its shape keeping axisymmetry. The same applies for the configuration with the nonporous tube, with expansion being almost negligible (only in the entrainment zone). Nevertheless, when open-sided tubes are used, the spout does not expand following axisymmetry, but it is more pronounced in the opened area of the draft tube. Furthermore, as air velocity is increased the fountain core expands all over the length of the fountain, and takes almost the whole volume of the confiner at high air velocity.

Open-sided draft tubes have proven to be an essential internal device for the scaling up of spouted beds, since they confer great stability upon the system and, furthermore, provide additional gas-solid contact

in the fountain compared to that obtained in the configuration without tube. Nevertheless, they lead to changes in the spout-annulus interface in the bed and in the core-periphery interface in the fountain, which must be considered in any rigorous modelling of these gas-solid contact methods.

Nomenclature

AR	Aperture ratio, %
D_0	Gas inlet diameter, m
D_C	Column diameter, m
D_F	Diameter of the fountain confiner, m
D_i	Contactor base diameter, m
d_p	Average particle diameter, mm
D_T	Diameter of the draft tube, m
H	Measuring height, m
H_0	Static bed height, m
H_C	Height of the conical section, m
H_F	Distance between the bed surface and the lower end of the device, m
L_F	Length of the fountain confiner, m
L_H	Height of the entrainment zone of the draft tube, m
L_T	Height of the draft tube, m
r	Radius, m
r/R	Dimensionless radius
u	Velocity of the fluid, m s^{-1}
u_{ms}	Minimum spouting velocity at the inlet section, m s^{-1}
v_s	Solid velocity, m s^{-1}

Greek letter

γ	Contactor angle, °

Declaration of Competing Interest

The authors declare that they have no known competing financial interests or personal relationships that could have appeared to influence the work reported in this paper.

Acknowledgements

This work has received funding from Spain's Ministry of Science and Innovation (PID2019-107357RB-I00 (AEI/FEDER, UE)), the Basque Government (IT1218–19 and KK-2020/00107) and the European Commission (HORIZON H2020-MSCA RISE-2018. Contract No.: 823745). M. Tellabide thanks Spain's Ministry of Education, Culture and Sport for his Ph.D. grant (FPU14/05814). I. Estiati thanks the University of the Basque Country for her postgraduate grant (ESPDOC18/14).

References

[1] K. Mathur, N. Epstein, Spouted Beds, Academic Edition, Academic Press Incorporated, U.S., New York, 1974.
[2] M. Olazar, M.J. San José, A.T. Aguayo, J.M. Arandes, J. Bilbao, Stable operation conditions for gas-solid contact regimes in conical spouted beds, Ind. Eng. Chem. Res. 31 (7) (1992) 1784–1792, https://doi.org/10.1021/ie00007a025.
[3] F. Wu, J. Bai, J. Zhang, W. Zhou, X. Ma, CFD simulation and optimization of mixing behaviors in a spouted bed with a longitudinal vortex, ACS Omega 4 (5) (2019) 8214–8221, https://doi.org/10.1021/acsomega.9b00856.
[4] I. Estiati, A. Atxutegi, H. Altzibar, F. Freire, R. Aguado, M. Olazar, Multiple-output artificial neural network to estimate solid cycle times in conical spouted beds, Chem. Eng. Technol. (2021) https://doi.org/10.1002/ceat.202000491.
[5] R. Brito, R. Béttega, J. Freire, Energy analysis of intermittent drying in the spouted bed, Drying Technol. 37 (12) (2019) 1498–1510, https://doi.org/10.1080/07373937.2018.1512503.
[6] Q. Wang, X. Kong, H. Liu, G. Xiao, Combustion Experimental Study on Spouted Bed for Daqing Oil Shale Semi-Coke, Vol. 614-615, Advanced Materials Research, Germany, 2013 doi:10.4028/www.scientific.net/AMR.614-615.95.
[7] S. Orozco, J. Alvarez, G. Lopez, M. Artetxe, J. Bilbao, M. Olazar, Pyrolysis of plastic wastes in a fountain confined conical spouted bed reactor: determination of stable operating conditions, Energy Convers. Manage. 229 (2021) https://doi.org/10.1016/j.enconman.2020.113768.
[8] M. Cortazar, G. Lopez, J. Alvarez, M. Amutio, J. Bilbao, M. Olazar, Behaviour of primary catalysts in the biomass steam gasification in a fountain confined spouted bed, Fuel 253 (2019) 1446–1456, https://doi.org/10.1016/j.fuel.2019.05.094.
[9] B. Wu, A. Orta, A. Kantzas, Experimental flow measurements of a spouted bed using pressure transducer and X-ray CT scanner, Int. J. Chem. React. Eng. 9 (2011)https://doi.org/10.1515/1542-6580.2522.
[10] V. Mikhailik, The Pattern of change of spout diameter in spouting bed, Collected Works Res. Heat Mass Technol. Proc. 37 (1966) 37–41.
[11] M.A. Barrozo, C.R. Duarte, N. Epstein, J.R. Grace, C.J. Lim, Experimental and computational fluid dynamics study of dense-phase, transition region, and dilute-phase spouting, Ind. Eng. Chem. Res. 49 (11) (2010) 5102–5109, https://doi.org/10.1021/ie9004892.
[12] N. Ali, T. Al-Juwaya, M. Al-Dahhan, Demonstrating the non-similarity in local holdups of spouted beds obtained by CT with scale-up methodology based on dimensionless groups, J. Math. Psychol. 59 (2016) 129–141, https://doi.org/10.1016/j.cherd.2016.08.010.
[13] L. Godfroy, F. Larachi, G. Kennedy, B. Grandjean, J. Chaouki, On-line flow visualization in multiphase reactors using neural networks, Appl. Radiat. Isot. 48 (2) (1997) 225–235, https://doi.org/10.1016/S0969-8043(96)00183-2.
[14] L. Spreutels, B. Haut, R. Legros, F. Bertrand, J. Chaouki, Experimental investigation of solid particles flow in a conical spouted bed using radioactive particle tracking, AIChE J. 62 (1) (2015) 26–37, https://doi.org/10.1002/aic.15014.
[15] N. Ali, T. Al-Juwaya, M. Al-Dahhan, An advanced evaluation of spouted beds scale-up for coating TRISO nuclear fuel particles using Radioactive Particle Tracking (RPT), Exp. Therm. Fluid Sci. 80 (2017) 90–104, https://doi.org/10.1016/j.expthermflusci.2016.08.002.
[16] O. Gryczka, S. Heinrich, V. Miteva, N.G. Deen, J.A.M. Kuipers, M. Jacob, L. Mörl, Characterization of the pneumatic behavior of a novel spouted bed apparatus with two adjustable gas inlets, Chem. Eng. Sci. 63 (3) (2008) 791–814, https://doi.org/10.1016/j.ces.2007.10.023.
[17] M. Bieberle, F. Barthel, Combined phase distribution and particle velocity measurement in spout fluidized beds by ultrafast X-ray computed tomography, Chem. Eng. J. 285 (2016) 218–227, https://doi.org/10.1016/j.cej.2015.10.003.
[18] E.E. Patterson, J. Halow, S. Daw, Innovative method using magnetic particle tracking to measure solids circulation in a spouted fluidized bed, Ind. Eng. Chem. Res. 49 (11) (2010) 5037–5043, https://doi.org/10.1021/ie9008698.
[19] G. Mohs, O. Gryczka, S. Heinrich, L. M“orl, Magnetic monitoring of a single particle in a prismatic spouted bed, Chem. Eng. Sci. 64 (23) (2009) 4811–4825, https://doi.org/10.1016/j.ces.2009.08.025.
[20] M.J. San José, M. Olazar, R. Llamosas, M.A. Izquierdo, J. Bilbao, Study of dead zone and spout diameter in shallow spouted beds of cylindrical geometry, Chem. Eng. J. 64 (3) (1996) 353–359, https://doi.org/10.1016/S0923-0467(97)80006-1.
[21] I.D. Abdelrazek, Analysis of Thermo-Chemical Deposition in Spouted Beds, University of Tennessee, Knoxville, TN, 1969 Ph.D. thesis.
[22] M.A. Malek, L.A. Madonna, B.C. Lu, Estimation of spout diameter in a spouted bed, Ind. Eng. Chem. Proc. Des. Develop. 2 (1) (1963) 30–34, https://doi.org/10.1021/i260005a006.
[23] G.S. McNab, Predictions of spout diameter, Br. Chem. Eng. Proc. Tech. 17 (1972) 532.
[24] A. Benkrid, H.S. Caram, Solid flow in the annular region of a spouted bed, AIChE J. 35 (8) (1989) 1328–1336, https://doi.org/10.1002/aic.690350811.
[25] A.-L. He, C.J. Lim, J.R. Grace, S.-Z. Qin, Spout diameters in full and half spouted beds, Can. J. Chem. Eng. 76 (4) (1998) 702–706, https://doi.org/10.1002/cjce.5450760403.
[26] D. Roy, F.F. Larachi, R. Legros, J. Chaouki, A Study of solid behavior in spouted beds using 3-D particle tracking, Can. J. Chem. Eng. 72 (6) (1994) 945–952, https://doi.org/10.1002/cjce.5450720602.
[27] F. Wu, L. Shang, Z. Yu, X. Ma, W. Zhou, Experimental investigation on hydrodynamic behavior in a spouted bed with longitudinal vortex generators, Adv. Powder Technol. 30 (July) (2019) 2178–2187.
[28] H. Altzibar, G. Lopez, R. Aguado, S. Alvarez, M.J. San Jose, M. Olazar, Hydrodynamics of conical spouted beds using different types of internal devices, Chem. Eng. Technol. 32 (3) (2009) 463–469, https://doi.org/10.1002/ceat.200800605.
[29] M. Tellabide, I. Estiati, A. Pablos, H. Altzibar, R. Aguado, M. Olazar, New operation regimes in fountain confined conical spouted beds, Chem. Eng. Sci. 211 (2020) https://doi.org/10.1016/j.ces.2019.115255.
[30] A. Atxutegi, M. Tellabide, G. Lopez, R. Aguado, J. Bilbao, M. Olazar, Implementation of a borescopic technique in a conical spouted bed for tracking spherical and irregular particles, Chem. Eng. J. 374 (May) (2019) 39–48, https://doi.org/10.1016/j.cej.2019.05.143.
[31] C.R. M”uller, D.J. Holland, A.J. Sederman, J.S. Dennis, L.F. Gladden, Magnetic resonance measurements of high-velocity particle motion in a three-dimensional gas–solid spouted bed, Phys. Rev. E-Stat. Nonlinear Soft Matt. Phys. 82 (5) (2010) 1–4, https://doi.org/10.1103/PhysRevE.82.050302.
[32] G. Farnebäck, Fast and accurate motion estimation using orientation tensors and parametric motion models, Proceed. Int. Conf. Patt. Recogn. 15 (1) (2000) 135–139.
[33] G. Kulah, S. Sari, M. Koksal, Particle velocity, solids hold-up, and solids flux distributions in conical spouted beds operating with heavy particles, Ind. Eng. Chem. Res. 55 (11) (2016) 3131–3138, https://doi.org/10.1021/acs.iecr.5b04496.
[34] T. Djeridane, F. Larachi, D. Roy, J. Chaouki, R. Legros, Investigation of the mean and turbulent particle velocity fields in a spouted bed using radioactive particle tracking, Can. J. Chem. Eng. 76 (2) (1998) 190–195, https://doi.org/10.1002/cjce.5450760205.
[35] G.Q. Liu, S.Q. Li, X.L. Zhao, Q. Yao, Experimental studies of particle flow dynamics in a two-dimensional spouted bed, Chem. Eng. Sci. 63 (4) (2008) 1131–1141, https://doi.org/10.1016/j.ces.2007.11.013.
[36] M. Tellabide, I. Estiati, A. Atxutegi, H. Altzibar, R. Aguado, M. Olazar, Fine particle flow pattern and region delimitation in fountain confined conical spouted beds, J. Ind. Eng. Chem. 95 (2021) 312–324, https://doi.org/10.1016/j.jiec.2021.01.006.

[37] F.S. Castellana, B.A. Dudley, Imaging of particle motion in fluid-solid systems using a gamma camera, Chem. Eng. Commun. 29 (1-6) (1984) 113–123, https://doi.org/10.1080/00986448408940153.
[38] M. Olazar, M.J. San Jose, R. Llamosas, S. Alvarez, J. Bilbao, Study of local properties in conical spouted beds using an optical fiber probe, Ind. Eng. Chem. Res. 34 (1995) 4033–4039.
[39] H.C. Park, H.S. Choi, Visualization of flow structures inside a conical spouted bed by electrical capacitance volume tomography, Particuology 42 (2019) 15–25, https://doi.org/10.1016/j.partic.2018.01.002.
[40] X. Yang, J.R. van Ommen, E. Wagner, R.F. Mudde, Time-resolved characterization of a flat-base spouted bed with a high speed X-ray system, Chem. Eng. J. 254 (2014) 143–152, https://doi.org/10.1016/j.cej.2014.05.050.
[41] M. Al-Dahhan, S. Aradhya, H. Taofeeq, Prediction of spout diameter in gas-solid spouted beds using factorial design of experiments approach with the aid of advanced optical fibre probe, Can. J. Chem. Eng. 95 (8) (2017) 1463–1470, https://doi.org/10.1002/cjce.22817.
[42] Y.L. He, S.Z. Qin, C.J. Lim, J.R. Grace, Particle velocity profiles and solid flow patterns in spouted beds, Can. J. Chem. Eng. 72 (4) (1994) 561–568, https://doi.org/10.1002/cjce.5450720402.
[43] X. Chen, B. Ren, Y. Chen, W. Zhong, D. Chen, Y. Lu, B. Jin, Distribution of particle velocity in a conical cylindrical spouted bed, Can. J. Chem. Eng. 91 (11) (2013) 1762–1767, https://doi.org/10.1002/cjce.21850.
[44] M. Olazar, M.J. San José, M.A. Izquierdo, S. Alvarez, J. Bilbao, Fountain geometry in shallow spouted beds, Ind. Eng. Chem. Res. 43 (4) (2004) 1163–1168, https://doi.org/10.1021/ie030641d.
[45] M.J. San José, S. Alvarez, A. Morales, M. Olazar, J. Bilbao, Fountain geometry of beds consisting of plastic wastes in shallow spouted beds, Ind. Eng. Chem. Res. 47 (16) (2008) 6228–6238, https://doi.org/10.1021/ie071340x.
[46] M. Olazar, M.J. San José, S. Alvarez, A. Morales, J. Bilbao, Measurement of particle velocities in conical spouted beds using an optical fiber probe, Ind. Eng. Chem. Res. 37 (4) (1998) 4520–4527.
[47] M.J. San José, M. Olazar, S. Alvarez, A. Morales, J. Bilbao, Spout and fountain geometry in conical spouted beds consisting of solids of varying density, Ind. Eng. Chem. Res. 44 (1) (2005) 193–200, https://doi.org/10.1021/ie040137o.
[48] D.L. Pianarosa, L.A.P. Freitas, C.J. Lim, J.R. Grace, O.M. Dogan, Voidage and particle velocity profiles in a spout-fluid bed, Can. J. Chem. Eng. 78 (1) (2000) 132–142, https://doi.org/10.1002/cjce.5450780118.
[49] I.P. Mukhlenov, A.E. Gorstein, Investigation of a spouted bed, Kim. Prom. 41 (1965) 443–446.
[50] G. Volpicelli, G. Raso, L. Massimilla, Gas and solid flow in bidimensional spouted beds, Proceedings of the International Symposium on Fluidization 1967, p. 123.
[51] M. Green, J. Bridgwater, An experimental study of spouting in large sector beds, Can. J. Chem. Eng. 1 61 (1983) 281.